Ultramicroscopy 149 (2015) 86–94

Contents lists available at ScienceDirect

Ultramicroscopy

journal homepage: www.elsevier.com/locate/ultramic

Full Length Article

Imaging collagen type I fibrillogenesis with high spatiotemporal resolution

Dimitar R Stamov [a,*], Erik Stock [a], Clemens M Franz [b], Torsten Jähnke [a], Heiko Haschke [a]

[a] JPK Instruments AG, Bouchéstrasse 12, 12435 Berlin, Germany
[b] DFG-Center for Functional Nanostructures (CFN), Karlsruhe Institute of Technology (KIT), Wolfgang-Gaede-Strasse 1a, 76131 Karlsruhe, Germany

ARTICLE INFO

Article history:
Received 7 May 2014
Received in revised form
2 September 2014
Accepted 7 October 2014
Available online 28 October 2014

Keywords:
Collagen type I
Fibrillogenesis
Atomic force microscopy
AFM
Fast imaging

ABSTRACT

Fibrillar collagens, such as collagen type I, belong to the most abundant extracellular matrix proteins and they have received much attention over the last five decades due to their large interactome, complex hierarchical structure and high mechanical stability. Nevertheless, the collagen self-assembly process is still incompletely understood. Determining the real-time kinetics of collagen type I formation is therefore pivotal for better understanding of collagen type I structure and function, but visualising the dynamic self-assembly process of collagen I on the molecular scale requires imaging techniques offering high spatiotemporal resolution. Fast and high-speed scanning atomic force microscopes (AFM) provide the means to study such processes on the timescale of seconds under near-physiological conditions. In this study we have applied fast AFM tip scanning to study the assembly kinetics of fibrillar collagen type I nanomatrices with a temporal resolution reaching eight seconds for a frame size of 500 nm. By modifying the buffer composition and pH value, the kinetics of collagen fibrillogenesis can be adjusted for optimal analysis by fast AFM scanning. We furthermore show that amplitude-modulation imaging can be successfully applied to extract additional structural information from collagen samples even at high scan rates. Fast AFM scanning with controlled amplitude modulation therefore provides a versatile platform for studying dynamic collagen self-assembly processes at high resolution.

1. Introduction

Fibrillar collagen type I is the main component of different extracellular matrices (ECM), and one of the most abundant mammalian proteins [1]. For instance, it is preponderant in ligamentous and tendinous tissues, where it provides resilience to a range of uni- and multiaxial mechanical loads [2]. It is well-established that collagen I fibrils form in a hierarchical self-assembly process from molecular precursors, but five decades of collagen I research have seen different models describing the precise arrangement of these molecular building blocks in mature fibrils. In particular, there has been contrasting evidence regarding the crystallinity [3,4] and/or liquid-like disorder [5,6] of structural subdomains both on the molecular and fibrillar levels, which could be related to the unique mechanical properties of collagen [7].

A commonly accepted structural hierarchy of collagen starts with laterally staggered, triple-helical monomeric tropocollagen monomers (1.5 nm thick, 300 nm long), through microfibrillar units of 4–5 nm in diameter [8], to significantly larger nanometre/micrometre-sized fibrils [9]. One of the hallmarks of collagen I is its characteristic D-banding periodicity of 67 nm [10], resulting from the quarter-staggered alignment of collagen chains during fibrillogenesis [11]. The interactions that drive the self-assembly process are predominantly electrostatic and hydrophobic, with a suggested role of the D-band in optimal electrostatic pairing between neighbouring monomers, as well as in maximising contact between hydrophobic domain regions [12,13]. Further stabilisation mechanisms include molecular cross-links between the central triple-helical regions and short non-helical C- and N-terminal telopeptides [14].

Previous studies on collagen I kinetics suggest a multi-step process with a distinct nucleation (lag) phase and an exponential phase [15]. The nucleation phase is commonly associated with the formation of linear dimers and trimers with 4-D staggered monomeric collagen molecules. Such structures may then be further involved in the formation of macroscopic D-banded fibrils by means of lateral staggering [16]. The overall structure and dynamics of collagen I fibrillogenesis has been shown to be influenced by parameters such as temperature [17,18], pH value and salinity of the assembly solution [19–21], monomer concentration [22,23], or degree of telopeptide removal [24–26]. Additional fibrillogenesis

* Corresponding author. Tel.: +49 30 5331 12070; fax: +49 30 5331 22555.
E-mail address: stamov@jpk.com (D. Stamov).

http://dx.doi.org/10.1016/j.ultramic.2014.10.003
0304-3991/

regulatory mechanisms involve molecular interactions with other molecules, such as glycosaminoglycans [27–29], proteoglycans [30–32], or other types of collagen [33–35].

The last few decades have seen a strong demand for novel collagen I-based tissue engineering scaffolds. There have also been great efforts to elucidate the molecular mechanisms behind a number of collagen I-related anomalies and diseases [36]. However, given the structural heterogeneity of tissues, it is often difficult to determine the individual effect of specific parameters on the kinetics of collagen type I fibrillogenesis. This has led to an increase of *in situ* studies featuring different artificial model systems to study molecular mechanisms during collagen I fibrillogenesis in detail. Structurally heterogeneous gels with random fibrillar orientations significantly deviate from the native alignment of collagen I structures [28] and often obstruct high-resolution structural analysis. An interesting alternative is a previously employed technique for creating aligned nanofibrillar collagen I matrices by employing the entropy-driven self-assembly on a muscovite mica substrate [37].

Studying the dynamics of complex macromolecular collagen I systems also requires suitable imaging methods offering both high spatial and temporal resolution. The past years have established the atomic force microscope (AFM) as an indispensable tool for high resolution structural analysis of biological samples under physiological conditions [38]. Unlike other high-resolution imaging techniques, such as advanced electron microscopy and super-resolution optical microscopy, AFM does not usually demand specific sample modification and therefore does not introduce preparation artefacts. In addition, ongoing developments in fast and high speed AFM scanning are establishing this technique as a tool to look beyond individual snapshots of cellular processes or macromolecular assemblies, and to use it for studying dynamic biological systems with high temporal resolution as well [39–41].

Here, we report on the application of fast AFM imaging to reveal the dynamics of collagen type I fibrillogenesis with a temporal resolution reaching eight seconds per image frame. By modifying the concentration, pH and ion concentration of the working solution, we are furthermore able to look beyond the characteristic timeframe of conventional AFM imaging for collagen I fibrillogenesis and D-banding formation. In future, the applied experimental setup in combination with fast scanning could also be used for gaining novel insight into the dynamics of other macromolecules and biological systems with high spatial and temporal resolution.

2. Materials & methods

2.1. Buffer composition and reconstitution of collagen type I

For static experiments collagen type I nanomatrices were prepared by gluing mica discs (Ø 5–15 mm) to a microscope slide. A custom-made open fluid chamber was created by sealing a glass ring (Ø 21 mm) around the mica disk. Immediately before collagen reconstitution the mica substrates were cleaved to produce atomically flat surfaces suitable for high-resolution imaging. After the chamber was pre-filled with 50 mM L-glycine buffer (pH 9.2, containing 200 mM KCl), monomeric bovine collagen type I (PureCol, Advanced Biomatrix) stock solution (consisting of a high purity pepsin-extracted atelo-collagen) was injected to reach a desired total solution concentration between 15 and 100 μg/ml. Depending on the total collagen solution concentration, incubation times were varied between 1 h (100 μg/ml) and overnight (15 μg/ml). Following the reconstitution of collagen I at room temperature, the samples were shortly rinsed in glycine buffer to remove any unbound collagen and imaged immediately in buffer.

For studying collagen I dynamics, the custom-made chambers described above were pre-filled with imaging buffer solution. The tested buffer compositions included: 1) 50 mM L-glycine buffer (pH 9.2, 200 mM KCl); 2) Phosphate buffered saline (PBS) (pH 7.4, 10 mM phosphate buffer, 2.7 mM KCl, 137 mM NaCl); and 3) PBS + 200 mM KCl (pH 7.3). The buffer solutions were equilibrated for at least 30 min to minimise thermal drift. Finally, a calculated volume of monomeric collagen I stock solution was injected into the imaging solution directly on the mica substrate to reach the desired total solution concentration.

2.2. Fast-scanning atomic force microscopy (AFM)

Samples were analysed using a NanoWizard® ULTRA Speed AFM (JPK Instruments, Germany) mounted either on an inverted Nikon Eclipse TE2000-U optical microscope, or equipped with a JPK TopViewOptics™. Hydrated samples were imaged in buffer at ambient temperature in amplitude-modulation AC mode. For dynamic and static measurements we used fast-scanning high-resonant ultra-short cantilevers (USC-F0.3-k0.3, NanoWorld, Switzerland) with a nominal resonance frequency of 300 kHz in air, spring constant of 0.3 N/m, reflective chromium/gold-coated silicon chip, and high-density carbon tips with a radius of curvature of 10 nm.

2.3. Image processing and data analysis

AFM images were analysed with the native JPK DataProcessing software. When required, images were subjected to a polynomial surface tilt to correct for sample slope and/or flattened with a polynomial/histogram line-fit. Low-pass Gaussian and/or median filtering was applied to remove minor noise from the images. The Z-colour scale in all images is given as relative after processing, with the offset being kept the same within each of the figures to emphasise the structural features. This allows for the comparison of the same channels within each figure, but should not be taken as an absolute for comparing the absolute height values in the different figures. Particle thresholding analysis to calculate fibrillar coverage area was carried out with SPIP 6.2.4 (Image Metrology A/S). Preparation of supplementary movies and further analytical operations were carried out with ImageJ 1.48v. Graphical plotting and figure preparation was carried out with SciDAVis 0.2.4 and Inkscape 0.48.4. 2D spatial autocorrelation analysis was carried out by analysing the previously processed AFM height images with WSxM 5.0 Develop 6.5 software [42] with further normalisation.

3. Results

3.1. Resolving the characteristic D-band of collagen type I at different line rates

Studying fast dynamic processes, such as collagen type I fibrillogenesis *in situ*, requires the application of imaging techniques with high spatial and temporal resolution. Previous studies have shown that nanoscopic collagen I matrices can be reconstituted on mica substrates for high resolution AFM imaging [43]. When assembled in 50 mM glycine buffer containing 200 mM KCl at pH 9.2, these matrices contain a regular array of aligned collagen I nanofibrils. In this case the addition of potassium ions promotes the formation of a regular D-Band [44]. While these artificial matrices are highly suitable to reveal ultrastructural details of the fibrillar collagen assemblies, they are rather soft and prone to easy reorganisation by lateral forces exerted by the AFM tip during scanning [37,45], thus limiting the maximum AFM scan speed. However, studying dynamic collagen assembly requires the application of high imaging

line rates to capture transient structural differences during the evolution of collagen I fibrils, as well as a fast feedback system to track weak and rapidly changing signals such as the formation of collagen I intermediates. To test that the applied line rate had no adverse effect on image quality, the characteristic collagen type I banding of 67 nm was resolved while gradually increasing the imaging line rates from 5 Hz to about 30 Hz (Fig. 1).

The height images (A-F) show that the D-band can be resolved without apparent loss in image quality and specifically without introducing noticeable artefacts during imaging at all imaging speeds. Sub-20 nm collagen intermediates straying away from the main fibrillar structures could also be observed. Comparison of images acquired at different line-rates shows that it is even possible to resolve sub-D-banding periodicities of collagen I in all cases. The overall acquisition time for a single image of 512 × 512 pixels at a line rate of 30 Hz (Fig. 1F) is close to 17 seconds per frame. This is a significant reduction to the previously reported acquisition times of about 4–5 min per frame [43], and, therefore, a promising advancement for studying collagen kinetics with higher temporal resolution.

3.2. Varying the imaging setpoint unveils different structural levels of collagen I

Studying soft and fragile collagen I films requires a precise force control and fast system tracking feedback to observe even small morphological differences, as well as to ensure stable imaging. To evaluate imaging stability during long-term scanning, a fully reconstituted collagen type I film was imaged at a line-rate of 30 Hz over a sequence of 88 frames, while varying the setpoint during imaging (Fig. 2).

Overall, scanning remained stable over the entire imaging period, but the application of different imaging setpoints modulated the tip-sample interaction, revealing different structural hierarchical levels characteristic for collagen type I. All obtained height images provide high-resolution structural information about the size and distribution of inner monomeric and oligomeric building blocks present in collagen type I fibrils (Fig. 2A-D). Phase images provide further details about two sets of structural information – the molecular organisation within the fibrillar collagen film, as well as the sub-D-banding periodicity arising from the staggering/packing of monomeric/oligomeric collagen type I molecules (Fig. 2E-H). In additional experiments, we verified that the collagen ultrastructure was unaffected by the amplitude setpoint variation during imaging, as rescanning a larger area containing the original imaged area revealed no apparent structural differences to the collagen layer (see supplementary video 2).

3.3. Early formation of crimp/ribbon-like structures at pH 9.2

After having established that collagen fibrils could be stably imaged by continuous fast AFM scanning, we applied this technique to further dynamic studies of the collagen fibrillogenesis. Similar to the static conditions with fully reconstituted collagen type I nanomatrices (Fig. 2), dynamic imaging of collagen type I was carried out in glycine buffer, but in this case, after injecting monomeric solution directly on the mica surface. Such an approach enables the observation of collagen I fibrillogenesis taking place directly at the mica/buffer interface. Under these conditions collagen I was forming crimped ribbon-like structures (Fig. 3), as previously reported by Jiang et al. [44].

Consecutive dynamic sets were then recorded with a temporal resolution of 10–14 s per frame over a period of 4 h (Fig. 3A-E). The D-band became apparent already after 15–17 min of fibrillogenesis on the mica substrate (see supplementary video 3). Initially, the fibrillar intermediates assumed a random orientation on the substrate (Fig. 3A,B), but gradually started to fuse into larger collagen I fibrils after 90–120 min (Fig. 3C-E), and eventually resulted in a dispersed matrix of aligned ribbon-like collagen I fibrils (Fig. 3F). Interestingly, such structures were sparser than in fully reconstituted matrices

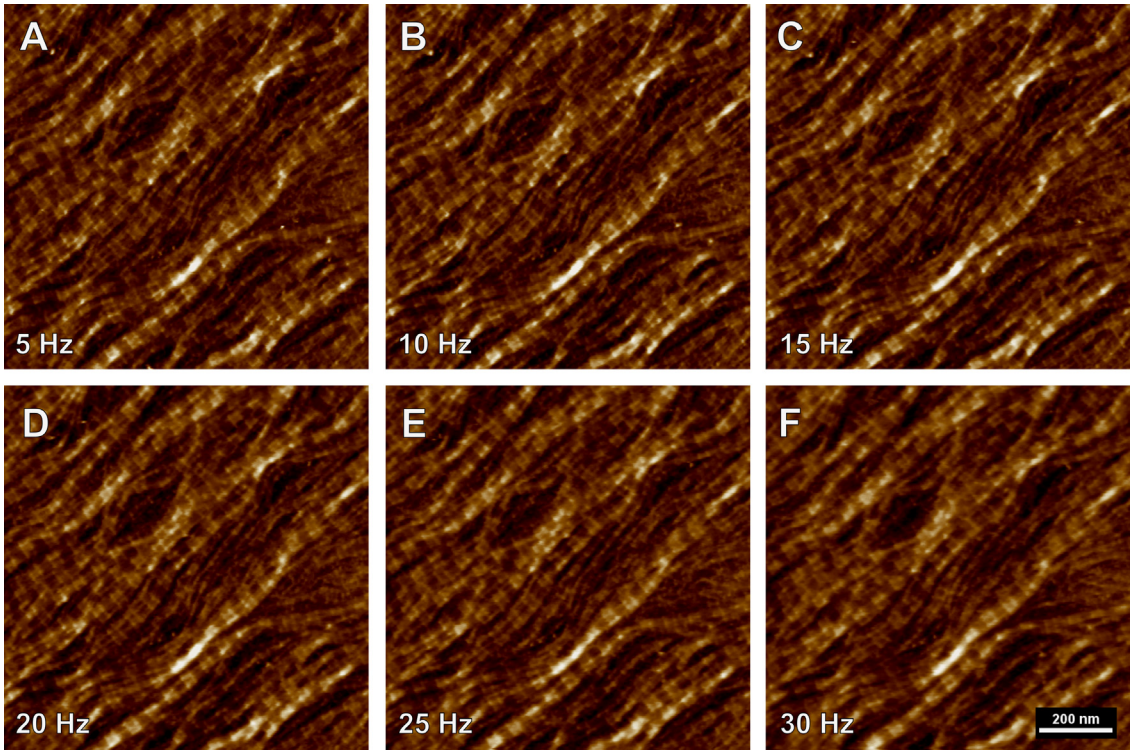

Fig. 1. Collagen type I banding periodicity observed at different line rates. Reconstitution of collagen type I was carried out in glycine buffer (pH 9.2), followed by rinsing and imaging in PBS buffer (pH 7.4) at ambient conditions (see Materials & Methods for complete buffer compositions). (A-F) AFM Height channels show that the D-periodicity of collagen I can be resolved without apparent loss in quality of its sub-banding structure at different line rates, resulting in acquisition times of down to 17 s per frame. Scan size is $1 \times 1\ \mu m$ with a resolution of 512 × 512 pixels (Height scale in A-F is 8 *nm*).

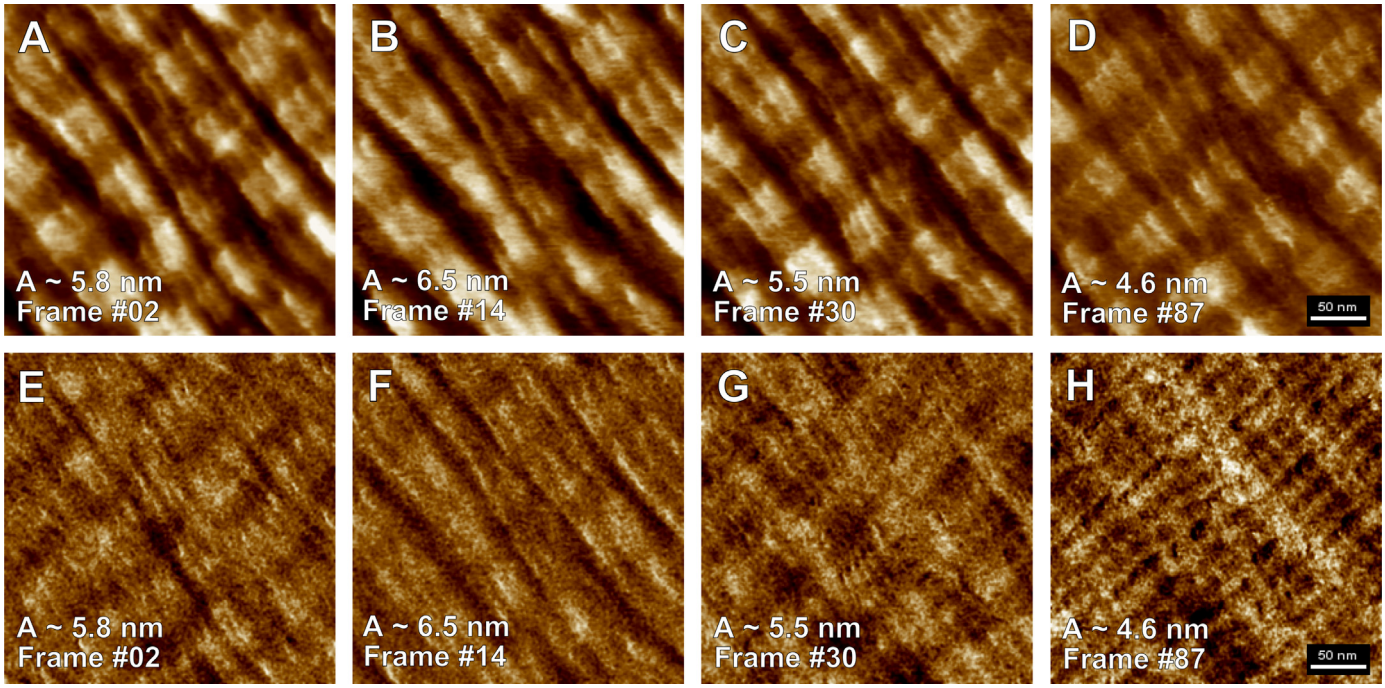

Fig. 2. Hierarchical organisation of collagen type I revealed by modulation of the setpoint amplitude. Collagen type I fibrils, previously reconstituted overnight under ambient conditions at a total solution concentration of 30 μg/ml (in 50 mM Glycine-buffer with 200 mM KCl, pH 9.2) were imaged in amplitude-modulation AC mode. The overall sequence of 88 frames was recorded using a USC cantilever at a scan size of 300 nm with a resolution of 256 × 256 pixels and a line rate of 30 Hz, resulting in an image acquisition time of 8.5 s per frame (for full sequence see supplementary video 1). Representative height (A-D) images acquired at four different setpoints give information about the molecular building blocks characteristic for the collagen type I fibrils. For informative purposes and better representation, the amplitude setpoint was converted into *nm*, by applying an empirical value for the sensitivity of the USC cantilevers (7 *nm*/V - from previous experience). Corresponding phase images (E-H) show that decreasing the setpoint by 0.9 *nm* can reveal different structural levels, i.e. individual molecular segments seen at 5.5 *nm* (G) and sub-D-periodic collagen banding as observed at 4.6 *nm* (H). Z-scales in (A-D) and (E-H) are 10 *nm* and 3 degrees respectively.

observed previously after overnight (12–16 h) incubation at the same total solution monomeric collagen concentration of 30 μg/ml (Fig. 2), suggesting slower overall dynamics of *in situ* assembled fibrils. A closer look at the growing tips of collagen type I fibrils showed that the assembly process is mediated by longitudinal step-wise addition of single building blocks protruding from the main fibrillar body (see supplementary Figure S1, compare A/B and B/C). The image sequence provides further information about the step-wise formation of the D-band with time. The overall linearity of the collagen type I segments was assessed by autocorrelating the representative frames given in Fig. 3 (for more details, see Supplementary Figure S2) and demonstrates a time-dependent increase of fibrillar alignment and change of orientation at these conditions.

3.4. Kinetics of collagen type I fibrillogenesis at physiological pH

The importance of pH for collagen I fibrillogenesis *in vitro* have been emphasised previously [46]. Fibril assembly at pH 9.2, was previously suggested as optimal for minimisation of assembly defects and applied to produce a homogenous collagen layer particularly suitable for high-resolution analysis [37]. However, obtaining physiologically relevant information regarding collagen I fibrillogenesis requires similar pH values as present in the extracellular environment of eukaryotic cells. Therefore, we studied the dynamic reconstitution of collagen type I in PBS buffer containing 2.7 mM KCl at physiological pH (7.4). Unlike reconstitution in glycine buffer at pH 9.2 at similar overall monomeric concentration of 30 μg/ml, in this case the surface was covered with fibrils already within 3–4 min after the start of the imaging (Fig. 4), demonstrating a significantly enhanced assembly rate.

The assembly process started with the formation of 300–600 *nm* long seemingly oligomeric structures (Fig. 4B) which further grew into both longitudinal and lateral directions (Fig. 4D-I). After normalising the relative covered area with respect to image size, it is possible to plot normalised surface coverage vs. reconstitution time, and thus the kinetics of collagen I fibrillogenesis (Fig. 4C). The data points from the relation were fitted with a Boltzmann sigmoidal equation, which allows for a clear separation of the nucleation and the exponential kinetics phase. Such results demonstrate that the enhanced collagen kinetics at physiological pH can be studied by fast AFM scanning even when using comparatively high starting monomer concentrations. It is therefore not necessary to significantly reduce the concentration in order to study native collagen I kinetics, as emphasised previously [47]. The absence of an apparent D-band under these conditions can be explained with the low potassium ion concentration of the PBS buffer.

3.5. Reconstitution of the D-band at physiological pH in presence of 0.2 M KCl

The importance of KCl for the reconstitution of the collagen I D-periodicity have been previously demonstrated [44,48]. To evaluate the influence of KCl on fibrillogenesis at physiological pH, we further reconstituted collagen type I in PBS buffer (pH 7.3) supplemented with 200 mM KCl. The presence of higher KCl concentrations appears to be essential for the D-periodicity (Fig. 5), confirming previous reports using buffers at different pH values [37,45].

In KCl-supplemented PBS buffer, fibril formation could be resolved with a temporal resolution of 8 s per frame (Fig. 5A-E). A fusing of adjacent fibrils becomes visible in Fig. 5C and is very apparent in Fig. 5E, and occurs at an angle of about 8–12 degrees between the fibril directions. The end of a growing tip in Fig. 5F-I shows a stepwise longitudinal addition of collagen I intermediates at a timescale of nearly 17 s per frame. A closer look at the main fibril in Fig. 5F-I shows that the characteristic twist of the collagen intermediates within the collagen fibrils already appears in sub-50 nm fibrillar structures.

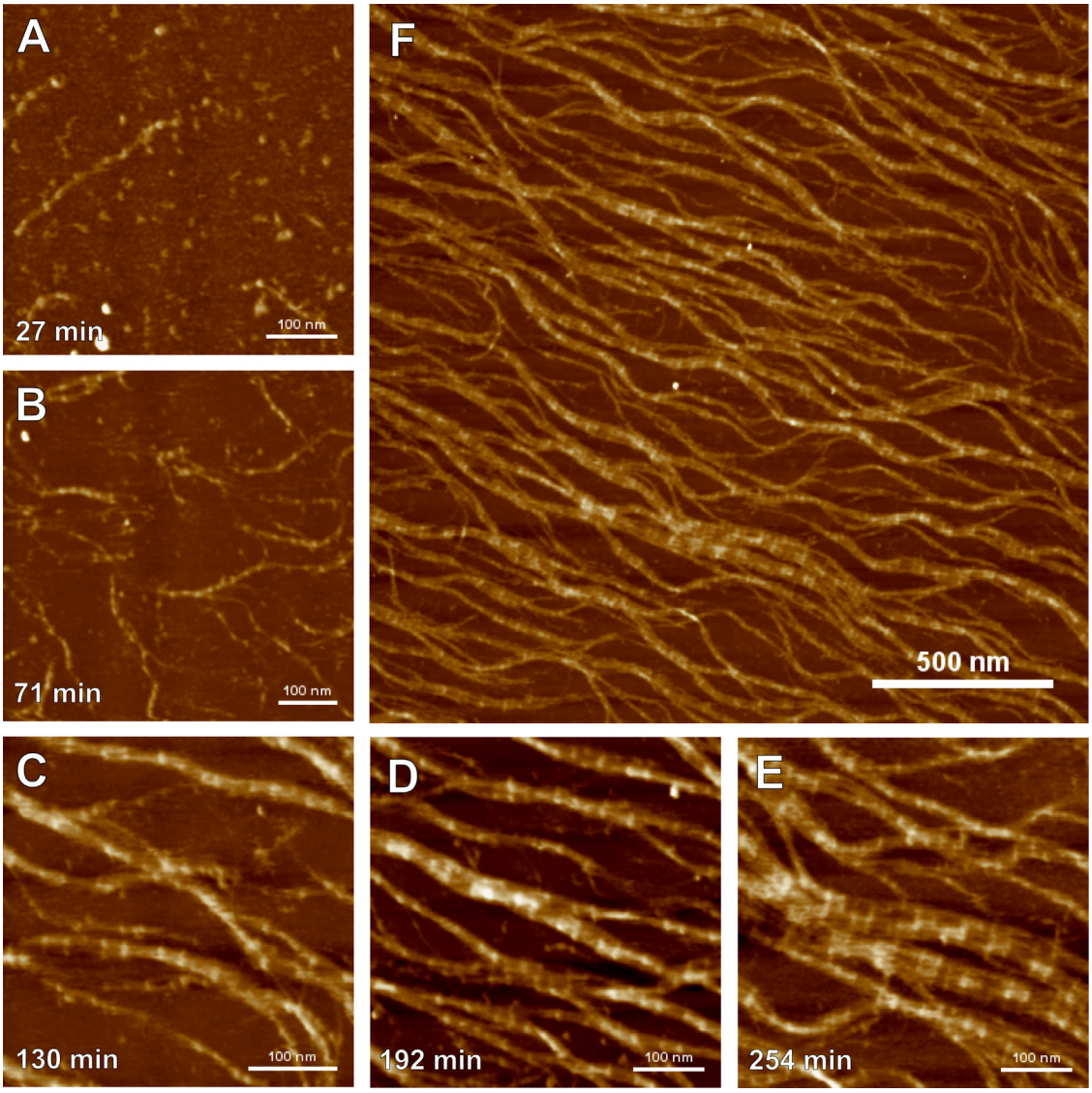

Fig. 3. Early dynamics of D-banded crimp-like fibrils at pH 9.2. Collagen type I fibrillogenesis was studied in 50 mM glycine buffer (containing 200 mM KCl, pH 9.2) at a total collagen monomer concentration of 30 μg/ml over a period of 4 h with a USC cantilever. Representative images from selected collagen I dynamics sets are given in (A-E). An overview image showing total surface coverage after the 4 h of AFM imaging of fibrillogenesis is given in (F). Image scan size in (C), (A, D, E), (B) and (F), is 400 *nm*, 500 *nm*, 600 *nm* and 2 *μm* respectively. Pixel resolution in (A-E) and (F) is 256×256 and 512×512 pixels respectively. Z-height in all images is 5 *nm*. Timestamps are recalculated respective to the injection time. Sequences of each representative set are available as part of a composite supplementary video 3.

The characteristic D-periodicity of collagen I results from the axial packing arrangement of collagen monomers in the fibrils [49]. By combining fast scanning rates and high pixel resolution it was further possible to resolve part of the inner D-band structure of collagen I staggering (Fig. 6).

Images were recorded with high spatial resolution on the timescale of about 2 min. These conditions therefore minimise conventional AFM problems, such as thermal drift and subsequent introduction of morphological artefacts, during scanning.

4. Discussion

The aim of the study was to gain a deeper insight into the dynamics of collagen type I fibrillogenesis by applying fast AFM scanning to a previously reported *in situ* system for collagen self-assembly [50]. We first verified that neither mechanical interactions during imaging nor elevated scanning speeds introduce morphological artefacts. A further focus was put on adjusting the kinetics of collagen I fibrillogenesis using buffers with different composition, pH values, and potassium ion concentration for optimal matching with the timeframe provided by fast AFM scanning.

AFM images of reconstituted collagen I fibrils recorded at increasing line rates of 5 to 30 Hz showed that higher tip velocities do not compromise the quality of the collagen I images (Fig. 1). 512 pixel images recorded at a near 30 Hz line rate resolved both the characteristic D-periodicity of collagen I, as well as sub-20 nm collagen I fibril tips with no apparent loss in imaging quality (Fig. 1F). Images recorded at 30 Hz line rate have a temporal resolution of 17 s, which is a significant improvement over previously recorded 5 min per frame in kinetic studies at similar pixel resolution [43]. Such conditions represent more closely the dynamics of macromolecular *in vitro* or *in vivo* systems which typically feature much higher collagen I concentrations [22] and could easily take place on a much shorter timescale. The high imaging stability, as demonstrated in Fig. 2 and Supplementary video 1, is in this case of particular importance for monitoring even small morphological

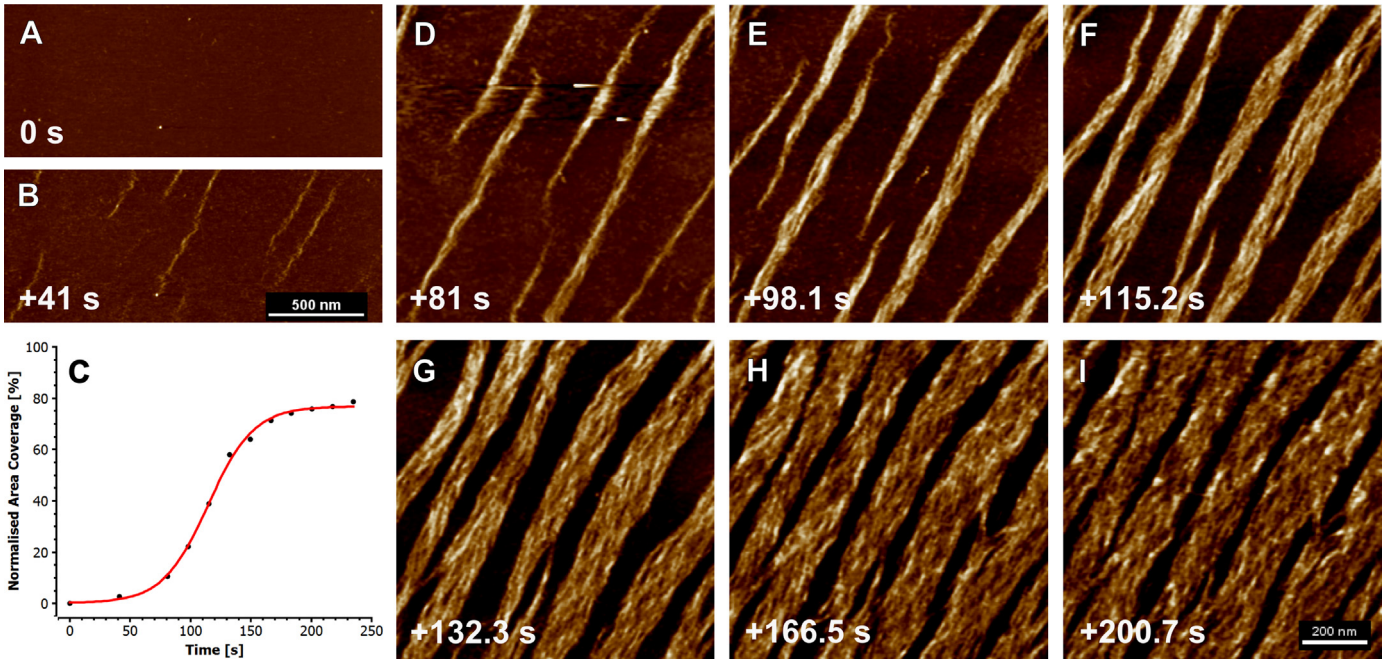

Fig. 4. Collagen kinetics observed at physiological pH. Collagen type I fibrillogenesis in PBS buffer (standard) with pH 7.4 and monomer concentration of 30 μg/ml was imaged at the mica interface with a USC cantilever. The timestamps are relative to the beginning of the imaging in (A) (t_0). (B) represents the formation of initial 300–600 *nm* long oligomeric intermediates of collagen type I with no D-banding which were formed within 41 s after the start of the imaging. (D-I) are representative frames of a consecutive set recorded at a line rate of 15 Hz (resolution of 256 × 256 pixels) over the original image location in (A) and (B) (before cropping) to reach a higher spatial resolution of the dynamic process. (C) is a Boltzmann-sigmoidal fit of the dynamic coverage of the imaged area with collagen fibrils within the first 12 frames, representing the two characteristic phases of collagen I kinetics – nucleation and exponential phase. The different area size in (A) and (B) was normalised and plot together with the relative covered area in the next 10 frames. X-scan size in (A, B) and (D-I) is 2 and 1 μm respectively, with a Z-height for all images of 3 *nm*. The full sequence starting with (D) is available as a supplementary video 4.

differences in dynamic systems such as collagen type I fibrillogenesis. Even at the applied line rate of 30 Hz, the internal structure of collagen I fibrils is easily resolved (Fig. 2A-D), depicting interdispersed individual collagen chains and the spacing between them. A reduction of the setpoint amplitude, which results in higher tip-sample interaction forces during AC mode, is a convenient tool for studying the different levels of structural organisation in collagen I fibrils. Step-wise setpoint reduction by approximately 1 *nm* each reveals a total of three different structural states, which is particularly obvious in the phase channel, being much more sensitive to the tip-sample interaction forces. A comparison of Fig. 2F-H shows the overall morphology (Fig. 2F), subsequent intermolecular packing of single collagen intermediates (Fig. 2G), as well as the sub-D-banding collagen I structure resulting from the lateral staggering and coordinated packing of amino acids from collagen I monomers (Fig. 2H). The temporal resolution during imaging was 8.5 s per frame.

Results from the dynamic studies with monomeric solution of collagen type I reconstituted in glycine buffer containing 200 mM KCL at pH 9.2, which was also used for the static imaging of reconstituted collagen I nanolayers, showed that the kinetics of the process at a total solution concentration 30 μg/ml is substantially slower in comparison to previously reported reconstitution times [43]. The time-dependent formation of microribbon-like structures was studied over a period of 4 h, and showed that within the first 30–60 min the small collagen I intermediates have a random orientation. After the initial 60–90 min, molecules were observed to fuse and eventually straighten. The D-banding of the collagen fibrils could be clearly distinguished after the first 120 min. Further fusion of collagen molecules eventually led to a more apparent straightening. The rather slow kinetics of this process explains why it took overnight incubation (12–16 h) at room temperature for the collagen I layer to cover the surface completely. It appears that at these conditions the gradual fusing of dispersed collagen I molecules leads to a full straightening of the reconstituted layers after longer periods of time (Fig. 2). Previous reports have shown that an increase in ionic strength (I) of the KCl solution from 10^{-4} M to 10^{-2} M significantly reduces the isoelectric point (IEP) of collagen fibrils from pH 7.5 to 5.3 [51]. This has a profound effect on the overall net charge of collagen fibrils, making them more acidic (negatively charged). The negatively charged mica surface could therefore easily hinder the kinetics of fibrillogenesis due to the lower number of nucleation sites. The change from a random to aligned orientation on the surface is expected to arise from the subsequent molecular staggering of the collagen molecules into bigger D-banded fibrils (Fig. 3C-F, and supplementary video 3). The fibrillogenesis snapshots after about 4 h of reconstitution at pH 9.2 (200 mM KCl) (Fig. 3F) and 12–16 h (Fig. 2) corroborate that observation. The noticeable difference with a previous result using the same artificial system may easily arise from the different inoculation technique, which in our case was being carried out directly on the substrate, versus pre-nucleation in a rather small bulk collagen solution volume (prone to rather heterogeneous effective surface concentrations) [43]. Additionally, different protein purification or storage protocols, affecting the intactness of the full amino acid sequence of the collagen monomers, can also account for a different surface charging, hence different IEP of collagen I in the experimental setup [52]. Further reasons can also feature the different mica source used as compared to previous studies.

Switching to a different buffer solution (PBS, 2.7 mM KCl, pH 7.4) and significantly lower ionic strength is expected to result in a more positive net charging of the collagen I molecules. As shown in Fig. 4 the kinetics of the assembly process on mica is very fast and follows the typical longitudinal growth of the collagen fibrils in the early nucleation phase. During transition to the exponential phase, the collagen I kinetics is expected to follow a sigmoidal increase in solution density (amount of light-scattering molecules)

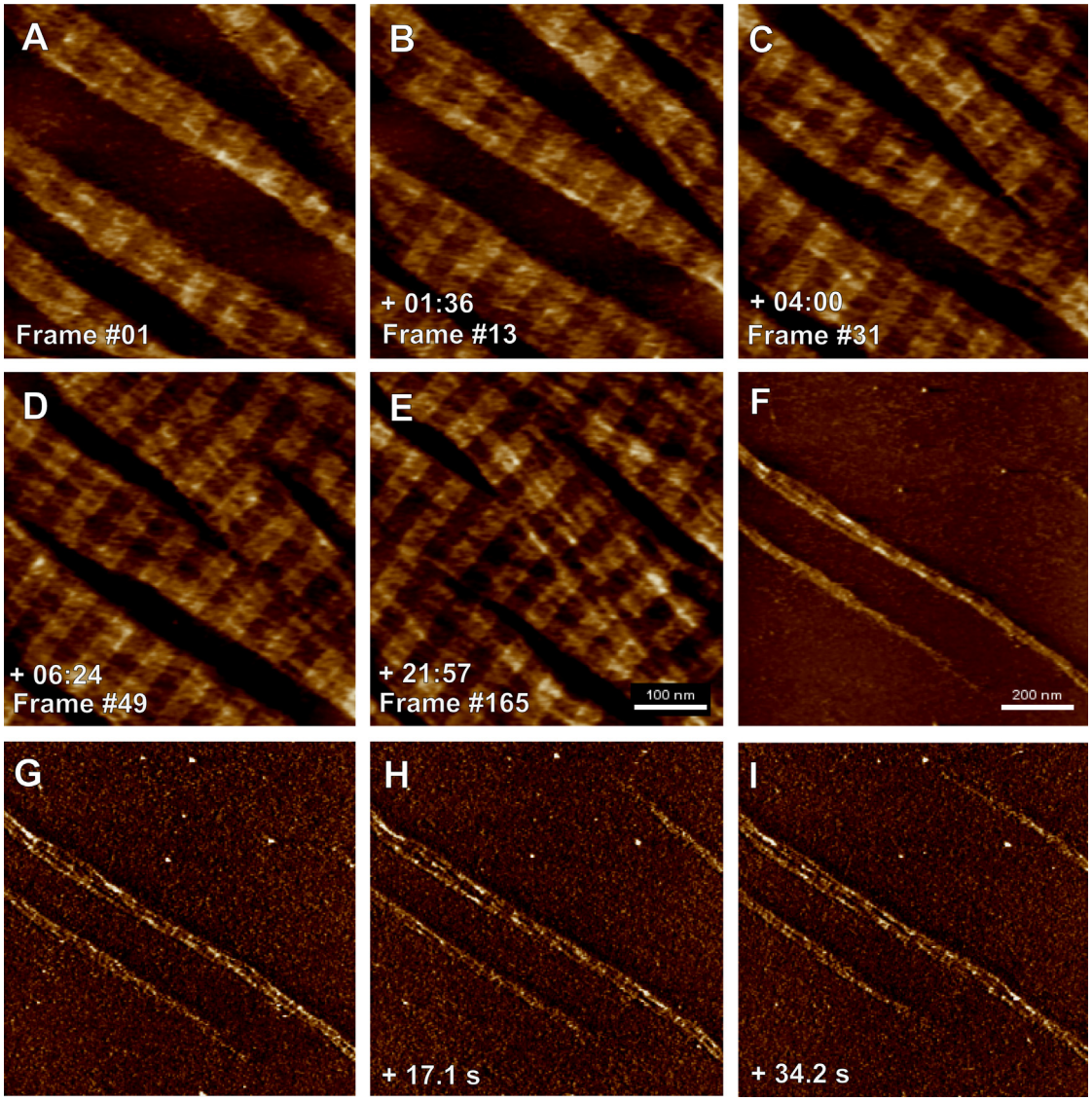

Fig. 5. Collagen type I fibrillogenesis observed at pH 7.3 (PBS buffer, 0.2 M KCl). (A-E) AFM Height images of D-banded collagen type I fibrils reconstituted in PBS buffer (pH 7.3) that was additionally supplemented with 200 mM KCl. (A-E) are representative frames of a full set of 166 consecutive images recorded at 32 Hz line rate and resolution of 256 × 256 pixels (timescale of 8 s per frame). (F) and (G) are the height and phase channel of a frame depicting the growth of a sub-50 *nm* collagen fibril. (G-I) show 3 consecutive phase images of a growing collagen I tip. Image size in (A-E) and (F-I) is 500 *nm* and 1 μm respectively. Z-scales in (A-F) and (G-I) are 5 *nm* and 4 degrees respectively. Line rate in (F-I) is 15 Hz at resolution of 256 × 256 pixels. Timestamps correspond to the beginning of the imaging.

[15,16]. In agreement, after normalisation of the calculated surface area, surface coverage shows an exactly sigmoidal increase vs. fibrillogenesis/imaging time (Fig. 4C). To our knowledge this is the first reconstruction of the sigmoidal kinetic behaviour of collagen I with such high spatial and temporal resolution (timescale of 3–4 min) from real-time microscopy imaging. The surface coverage in that case is most likely affected by the availability of collagen monomers and the pH value of the solution, which in turn influence the overall kinetics of the collagen I fibrillogenesis [44]. Additional experimental parameters, such as buffer purity, efficiency of mica cleaving, or presence of salt crystals can further contribute to the only partial coverage of the surface with collagen I. The lack of D-banding confirms the importance of higher potassium ion concentration for the formation of the characteristic for collagen type I 67 *nm* periodicity, as emphasised previously [44]. In turn, supplementing PBS with 200 mM KCl has a dramatic effect on fibril formation, resulting in the appearance of the characteristic D-banding as seen by a set of consecutive images over an imaging timeframe of 22 min in Fig. 5A-E. The image sequence shows the lateral growth and fusion of fully D-banded collagen type I fibrils on the time-scale of 8 s per frame. The typical longitudinal growth of collagen type I also remains unaffected as seen from the short sequence of three frames in Fig. 5F, G-I. A closer look at Fig. 5F also shows that at a sub-50 *nm* level, collagen intermediates already exhibit the typical nanoscale rope-like structures suggested previously [11].

As emphasised earlier, the alignment and lateral staggering of collagen monomers determines the banding periodicity of fibrillar collagen I, which is driven by hydrophobic and electrostatic interactions governed by the amino acid sequence. In native molecules, the D-band periodicity is typically about 67 *nm* and exhibits an axial polarity which is a result of asymmetric amino acid composition and parallel staggering within the fibrils [12]. The intricate structure of the D-band further contains up to 12 sub-periods which can be discerned in electron microscopy images [49]. Interestingly, different collagen extraction/purification protocols [53], pH value and salinity [20], degree of telopeptide removal [26,54], and presence of glycosaminoglycans and proteoglycans [55] all have been shown to

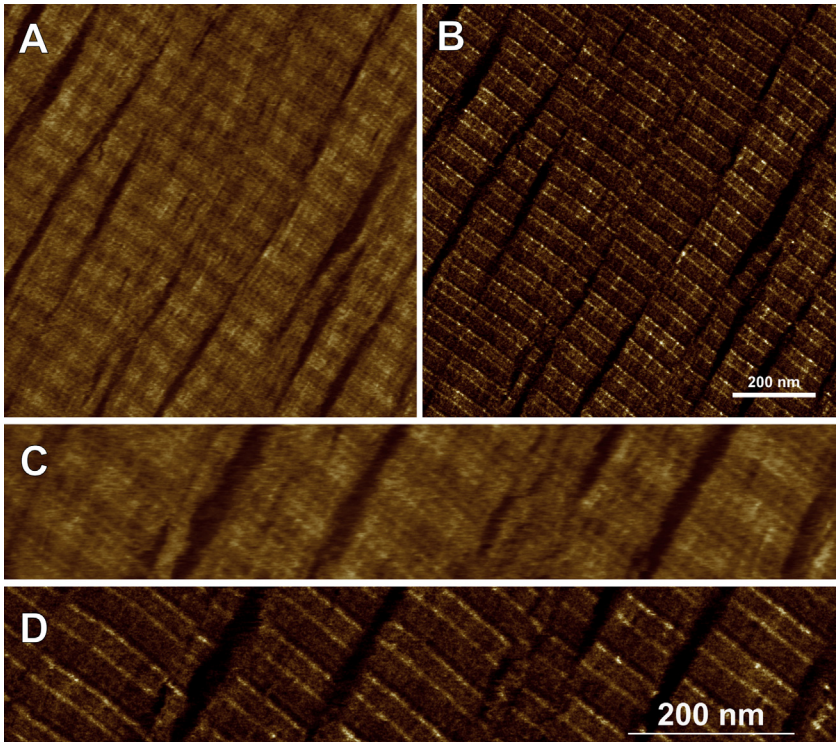

Fig. 6. Sub-D-periodic structure of collagen type I revealed by fast imaging. The sub-banding of collagen type I reconstituted in PBS buffer (+200 mM KCl) with pH 7.3 was recorded at 15 Hz and resolution of 2048 × 2048 (A, B) and 8192 × 1532 pixels (C, D) respectively. The times for recording the images were 136 s (A, B) and 102 s (C, D) respectively. X-scan size in (A, B) and (C, D) was 1 μm. Z-scale in the height (A, C) and phase (B, D) channels is 2 nm and 3 degrees respectively.

affect native monomer alignment. Variations in some of these factors may result in the formation of further banding periodicities known as polymorphic forms. Fast imaging with high spatial resolution (Fig. 6) is an intriguing possibility to observe D-band formation under different conditions in real time (Supplementary figure 1). It also provides the possibility to study fully reconstituted molecular matrices with high spatial resolution (Fig. 6C), which could be used as a molecular fingerprinting tool to verify monomeric arrangement and internal structure of collagen I-based *in vitro* and *in vivo* systems, as suggested previously [56].

5. Conclusions

We demonstrate that fast-scanning amplitude-modulation AFM can be successfully applied for real-time monitoring the kinetics of collagen I fibrillogenesis in an *in situ* system on atomically flat mica substrates. By demonstrating that there is no apparent loss in image quality with increase of the applied line rates and over long-term scanning, we can ascertain that the applied forces do not disturb the self-assembly of collagen I, enabling us to study fibril formation over at least 4 h. The imaging was carried out with high spatial and temporal resolution (reaching 8 s per frame), and in combination with different collagen assembly buffers. Our results show that the fastest rate of collagen I fibrillogenesis was recorded at near physiological pH in PBS buffer. We further emphasise the importance of sufficient potassium ions for the reconstitution of the 67 *nm* D-periodicity of collagen I. The discussed artificial experimental system provides an interesting platform for future long-term and non-invasive studies of macromolecular assembly processes, in which individual assembly steps may occur on the timescale of seconds, but require monitoring for hours until completed.

Acknowledgements

The authors would like to thank Rachel Owen and Torsten Müller at JPK Instruments AG for inspiring discussions and the critical review during the preparation of the manuscript. Technical assistance from Florian Kumpfe with sample preparation is gratefully acknowledged.

Appendix A. Supporting information

Supplementary data associated with this article can be found in the online version at http://dx.doi.org/10.1016/j.ultramic.2014.10.003.

References

[1] K.E. Kadler, D.F. Holmes, J.A. Trotter, J.A. Chapman, Collagen fibril formation, Biochem. J. 316 (1996) 1–11.
[2] P. Fratzl, R. Weinkamer, Nature's hierarchical materials, Prog. Mater. Sci. 52 (2007) 1263–1334.
[3] D.J. Hulmes, J.C. Jesior, A. Miller, C. Berthet-Colominas, C. Wolff, Electron microscopy shows periodic structure in collagen fibril cross sections, Proc. Natl. Acad. Sci. U. S. A. 78 (1981) 3567–3571.
[4] J.C. Jésior, A. Miller, C. Berthet-Colominas, Crystalline three-dimensional packing is a general characteristic of type I collagen fibrils, FEBS Lett. 113 (1980) 238–240.
[5] R.D. Fraser, T.P. MacRae, A. Miller, Molecular packing in type I collagen fibrils, J. Mol. Biol. 193 (1987) 115–125.
[6] T.J. Wess, A.P. Hammersley, L. Wess, A. Miller, A consensus model for molecular packing of type I collagen, J. Struct. Biol. 122 (1998) 92–100.
[7] D.J. Prockop, A. Fertala, The collagen fibril: the almost crystalline structure, J. Struct. Biol. 122 (1998) 111–118.
[8] J.P.R.O. Orgel, T.C. Irving, A. Miller, T.J. Wess, Microfibrillar structure of type I collagen in situ, Proc. Natl. Acad. Sci. U. S. A. 103 (2006) 9001–9005.
[9] S. Perumal, O. Antipova, J.P.R.O. Orgel, Collagen fibril architecture, domain organization, and triple-helical conformation govern its proteolysis, Proc. Natl. Acad. Sci. U. S. A. 105 (2008) 2824–2829.
[10] B. Eyden, M. Tzaphlidou, Structural variations of collagen in normal and pathological tissues: role of electron microscopy, Micron 32 (2001) 287–300.

[11] L. Bozec, G. van der Heijden, M. Horton, Collagen fibrils: nanoscale ropes, Biophys J. 92 (2007) 70–75.
[12] D.J. Hulmes, A. Miller, D.A. Parry, K.A. Piez, J. Woodhead-Galloway, Analysis of the primary structure of collagen for the origins of molecular packing, J. Mol. Biol. 79 (1973) 137–148.
[13] F. Ortolani, M. Giordano, M. Marchini, A model for type II collagen fibrils: distinctive D-band patterns in native and reconstituted fibrils compared with sequence data for helix and telopeptide domains, Biopolymers 54 (2000) 448–463.
[14] N.C. Avery, T.J. Sims, A.J. Bailey, Quantitative determination of collagen cross-links, Method Mol. Biol. 522 (2009) 103–121.
[15] G.C. Wood, M.K. Keech, The formation of fibrils from collagen solutions. 1. The effect of experimental conditions: kinetic and electron-microscope studies, Biochem. J. 75 (1960) 588–598.
[16] F.H. Silver, R.L. Trelstad, Linear aggregation and the turbidimetric lag phase: type I collagen fibrillogenesis in vitro, J. Theor. Biol. 81 (1979) 515–526.
[17] W.D. Comper, A. Veis, The mechanism of nucleation for in vitro collagen fibril formation, Biopolymers 16 (1977) 2113–2131.
[18] K.E. Kadler, Y. Hojima, D.J. Prockop, Collagen fibrils in vitro grow from pointed tips in the C- to N-terminal direction, Biochem. J. 268 (1990) 339–343.
[19] D.L. Christiansen, E.K. Huang, F.H. Silver, Assembly of type I collagen: fusion of fibril subunits and the influence of fibril diameter on mechanical properties, Matrix Biol. 19 (2000) 409–420.
[20] J.R. Harris, A. Reiber, Influence of saline and pH on collagen type I fibrillogenesis in vitro: fibril polymorphism and colloidal gold labelling, Micron 38 (2007) 513–521.
[21] B.R. Williams, R.A. Gelman, D.C. Poppke, K.A. Piez, Collagen fibril formation. Optimal in vitro conditions and preliminary kinetic results, J. Biol. Chem. 253 (1978) 6578–6585.
[22] F. Gobeaux, G. Mosser, A. Anglo, P. Panine, P. Davidson, M.-M. Giraud-Guille, E. Belamie, Fibrillogenesis in dense collagen solutions: a physicochemical study, J. Mol. Biol. 376 (2008) 1509–1522.
[23] F.H. Silver, R.L. Trelstad, Type I collagen in solution. Structure and properties of fibril fragments, J. Biol. Chem. 255 (1980) 9427–9433.
[24] M. Brennan, P.F. Davison, Influence of the telopeptides on type I collagen fibrillogenesis, Biopolymers 20 (1981) 2195–2202.
[25] D. Helseth Jr, A. Veis, Collagen self-assembly in vitro. Differentiating specific telopeptide-dependent interactions using selective enzyme modification and the addition of free amino telopeptide, J. Biol. Chem. 256 (1981) 7118–7128.
[26] S.J. Leibovich, J.B. Weiss, Electron microscope studies of the effects of endo- and exopeptidase digestion on tropocollagen. A novel concept of the role of terminal regions in fibrillogenesis, Biochim. Biophys. Acta 214 (1970) 445–454.
[27] B. Obrink, A study of the interactions between monomeric tropocollagen and glycosaminoglycans, Eur. J. Biochem. 33 (1973) 387–400.
[28] D. Stamov, M. Grimmer, K. Salchert, T. Pompe, C. Werner, Heparin intercalation into reconstituted collagen I fibrils: impact on growth kinetics and morphology, Biomaterials 29 (2008) 1–14.
[29] G.C. Wood, The formation of fibrils from collagen solutions. 3. Effect of chondroitin sulphate and some other naturally occurring polyanions on the rate of formation, Biochem. J. 75 (1960) 605–612.
[30] T. Douglas, S. Heinemann, S. Bierbaum, D. Scharnweber, H. Worch, Fibrillogenesis of collagen types I, II, and III with small leucine-rich proteoglycans decorin and biglycan, Biomacromolecules 7 (2006) 2388–2393.
[31] S. Kalamajski, A. Oldberg, Fibromodulin binds collagen type I via Glu-353 and Lys-355 in leucine-rich repeat 11, J. Biol. Chem. 282 (2007) 26740–26745.
[32] P.J. Neame, C.J. Kay, D.J. McQuillan, M.P. Beales, J.R. Hassell, Independent modulation of collagen fibrillogenesis by decorin and lumican, Cell Mol. Life Sci. 57 (2000) 859–863.
[33] T. Minamitani, T. Ikuta, Y. Saito, G. Takebe, M. Sato, H. Sawa, T. Nishimura, F. Nakamura, K. Takahashi, H. Ariga, K. Matsumoto, Modulation of collagen fibrillogenesis by tenascin-X and type VI collagen, Exp. Cell Res. 298 (2004) 305–315.
[34] A.M. Romanic, E. Adachi, Y. Hojima, J. Engel, D.J. Prockop, Polymerization of pNcollagen I and copolymerization of pNcollagen I with collagen I. A kinetic, thermodynamic, and morphologic study, J. Biol. Chem. 267 (1992) 22265–22271.
[35] R.J. Wenstrup, J.B. Florer, E.W. Brunskill, S.M. Bell, I. Chervoneva, D.E. Birk, Type V collagen controls the initiation of collagen fibril assembly, J. Biol. Chem. 279 (2004) 53331–53337.
[36] J.-M. Bourhis, N. Mariano, Y. Zhao, K. Harlos, J.-Y. Exposito, E.Y. Jones, C. Moali, N. Aghajari, D.J.S. Hulmes, Structural basis of fibrillar collagen trimerization and related genetic disorders, Nat. Struct. Mol. Biol. 19 (2012) 1031–1036.
[37] D.A. Cisneros, J. Friedrichs, A. Taubenberger, C.M. Franz, D.J. Muller, Creating ultrathin nanoscopic collagen matrices for biological and biotechnological applications, Small 3 (2007) 956–963.
[38] D. Muller, AFM: A nanotool in membrane biology, Biochemistry 47 (2008) 7986–7998.
[39] T. Ando, N. Kodera, E. Takai, D. Maruyama, K. Saito, A. Toda, A high-speed atomic force microscope for studying biological macromolecules, Proc. Natl. Acad. Sci. U. S. A. 98 (2001) 12468–12472.
[40] T. Ando, T. Uchihashi, N. Kodera, High-speed AFM and applications to biomolecular systems, Annu. Rev. Biophys. 42 (2013) 393–414.
[41] L.M. Picco, L. Bozec, A. Ulcinas, D.J. Engledew, M. Antognozzi, M.A. Horton, M.J. Miles, Breaking the speed limit with atomic force microscopy, Nanotechnology 18 (2007) 044030.
[42] I. Horcas, R. Fernández, J.M. Gómez-Rodríguez, J. Colchero, J. Gómez-Herrero, A.M. Baro, WSXM: a software for scanning probe microscopy and a tool for nanotechnology, Rev. Sci. Instrum. 78 (2007) 013705.
[43] D.A. Cisneros, C. Hung, C.M. Franz, D.J. Muller, Observing growth steps of collagen self-assembly by time-lapse high-resolution atomic force microscopy, J. Struct. Biol. 154 (2006) 232–245.
[44] F. Jiang, H. Hörber, J. Howard, D.J. Müller, Assembly of collagen into microribbons: effects of pH and electrolytes, J. Struct. Biol. 148 (2004) 268–278.
[45] F. Jiang, K. Khairy, K. Poole, J. Howard, D.J. Müller, Creating nanoscopic collagen matrices using atomic force microscopy, Microsc. Res. Tech. 64 (2004) 435–440.
[46] J.R. Harris, A. Soliakov, R.J. Lewis, In vitro fibrillogenesis of collagen type I in varying ionic and pH conditions, Micron 49 (2013) 60–68.
[47] C.M. Franz, D.J. Muller, Studying collagen self-assembly by time-lapse high-resolution atomic force microscopy, Method. Mol. Biol. 736 (2011) 97–107.
[48] R.W. Loo, M.C. Goh, Potassium ion mediated collagen microfibril assembly on mica, Langmuir 24 (2008) 13276–13278.
[49] J.A. Chapman, M. Tzaphlidou, K.M. Meek, K.E. Kadler, The collagen fibril–a model system for studying the staining and fixation of a protein, Electron. Microsc. Rev. 3 (1990) 143–182.
[50] K. Poole, K. Khairy, J. Friedrichs, C. Franz, D.A. Cisneros, J. Howard, D. Mueller, Molecular-scale topographic cues induce the orientation and directional movement of fibroblasts on two-dimensional collagen surfaces, J. Mol. Biol. 349 (2005) 380–386.
[51] U. Freudenberg, S.H. Behrens, P.B. Welzel, M. Müller, M. Grimmer, K. Salchert, T. Taeger, K. Schmidt, W. Pompe, C. Werner, Electrostatic interactions modulate the conformation of collagen I, Biophys. J. 92 (2007) 2108–2119.
[52] Y. Li, A. Asadi, M.R. Monroe, E.P. Douglas, pH effects on collagen fibrillogenesis in vitro: Electrostatic interactions and phosphate binding, Mater. Sci. Eng. C. 29 (2009) 1643–1649.
[53] J.B. Lian, S. Morris, B. Faris, J. Albright, C. Franzblau, The effects of acetic acid and pepsin on the crosslinkages and ultrastructure of corneal collagen, Biochim. Biophys. Acta 328 (1973) 193–204.
[54] M.J. Capaldi, J.A. Chapman, The C-terminal extrahelical peptide of type I collagen and its role in fibrillogenesis in vitro, Biopolymers 21 (1982) 2291–2313.
[55] B.R. Olsen, Electron microscope studies on collagen. II. mechanism of linear polymerization of tropocollagen molecules, Z Zellforsch Mikrosk Anat. 59 (1963) 199–213.
[56] D. Stamov., K. Salchert, A. Springer, C. Werner, T. Pompe, Structural polymorphism of collagen type I–heparin cofibrils, Soft Matter 5 (2009) 3461–3468.